

Neonlike Ar and Cl $3p$ - $3s$ emission from a θ -pinch plasma

R. C. Elton

Naval Research Laboratory, Washington, D.C. 20375

R. U. Datla and J. R. Roberts

National Institute of Standards and Technology, Gaithersburg, Maryland 20899

A. K. Bhatia

NASA Goddard Space Flight Center, Greenbelt, Maryland 20771

(Received 17 April 1989)

Time-resolved extreme-ultraviolet emission from sixteen $3p$ - $3s$ transitions, some of the type in which lasing has been demonstrated in heavier elements, is measured for neonlike Ar^{8+} and Cl^{7+} . These observations are made on a hydrogen θ -pinch plasma with a 5% admixture of argon or freon (for Cl). Fourteen $3d$ - $3p$ spectral lines are also detected. The measured intensities are compared to theoretical predictions. All major lines agree within $\pm 30\%$. Hence, there is no evidence of anomalously intense lines originating on $2p^5 3p$ $J=2$ upper levels compared to $J=0$, as observed in gain experiments.

Major advances have been made in soft-x-ray lasing in the last few years. One very successful approach has been electron-collisional excitation pumping of $3p$ - $3s$ transitions in neonlike ions.^{1,2} Gain coefficients as large as 5 cm^{-1} have been deduced from measurements of the intensity as a function of length in elongated laser-produced plasmas for the six transitions labeled A - F in Fig. 1. The most extensive data are for Se^{24+} ions.² For the $2p^5 3p$ upper configuration in this ion, two $J=2$ levels have produced by far the largest intensities on the B and C transitions. This has been extremely puzzling, because the most recent modeling² predicts that the gain coefficient for the A transition should be as much as 1.7 times larger than

that of B . This translates to a predicted intensity for A greater than 5 times that for B . In fact, the A line was at first too weak to be unambiguously identified at all, while the B and C lasing lines were very intense.¹ In later experiments with an extended gain length, a relatively weak A line was observed.² Data on higher- Z neonlike ions² also indicate such a disagreement.

It is very important to ascertain whether or not this disagreement is associated with the detailed atomic kinetics which enter into the numerical codes that predict the strong A line. This is the purpose of the present experiment. Our approach is to compare measured (relative) intensities from spontaneous emission in a relatively low-density plasma with predictions of a numerical model and to search for any irregularities associated with excitation and decay processes.

Figure 2 shows the experimental setup. The experiment was conducted on the 50-kJ θ pinch at the National Institute of Standards and Technology. The details of the machine and the plasma diagnostics apparatus have been described elsewhere.^{3,4} This device has proven to be convenient, reproducible, stable, of large size, and of suitable plasma conditions for producing neonlike Ar^{8+} and Cl^{7+}

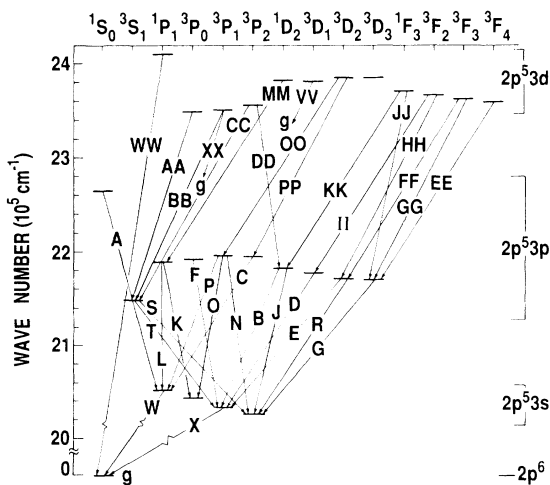


FIG. 1. Energy-level diagram of the $2p^6$ and $2p^5 3s$, $3p$, $3d$ configurations, labeled in LS -coupling notation. Alternate jj notation for the A - E transitions is given in the footnotes to Table I. All of the transitions shown were observed in this experiment.

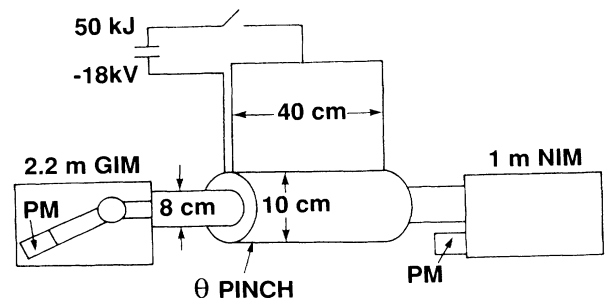


FIG. 2. Schematic of the experimental arrangement.

ions from gaseous mixtures. For these experiments, the total gas filling pressure was 22 mTorr. Of this, 2 mTorr was either argon gas or freon (CCl_2F_2) (for chlorine). The remainder was hydrogen. These were found to be optimum. Under these conditions recombination is negligible.³ An electron temperature of $kT_e = 65 \pm 6$ eV and an electron density of $N_e = (2.5 \pm 0.6) \times 10^{16} \text{ cm}^{-3}$ are determined by averaging the spatial profiles obtained for the time of interest by 90° Thomson scattering of ruby laser light.⁴ Variations in the radial direction over the region of interest are within the uncertainties quoted.

A 2.2-m grazing-incidence monochromator (GIM) and a 1-m normal-incidence monochromator (NIM) are aligned to view the plasma axially. Diaphragms limit the field of view of each to a 1.5-cm diameter cross section on axis. The GIM is equipped with a 1800-grooves/mm holographic grating. The resolution was adequate to separate the $n=3$ to $n=2$ soft-x-ray resonance lines used mainly for monitoring reproducibility. A 2400-grooves/mm high-resolution holographic grating was used in the NIM to resolve the closely spaced lines from $\Delta n=0$ transitions of interest. Both monochromators are equipped with a plastic scintillator and a photomultiplier for time-resolved measurements.

The radiometric calibration of the NIM was performed *in situ* using the branching-ratio technique.⁵ In this procedure, the ratio of intensities measured from two spectral lines from the same upper level and known transition probabilities yields the ratio of overall instrumental sensitivities at two wavelengths. The measured signals are then divided by the sensitivity at a particular wavelength to obtain the relative intensities. The spectral region between 447.8 and 529.9 Å was spanned with two spectral lines from O^{5+} ions originating on the $1s^2 4p^2 D$ upper term and terminating on $1s^2 3s^2 S$ and $1s^2 3d^2 D$ lower terms, with transition probabilities⁶ of 3.1×10^9 and $6.1 \times 10^8 \text{ sec}^{-1}$, respectively. This calibration was extended to longer wavelengths with two lines from O^{4+} ions at 529.33 and 739.8 Å. These share a common $1s^2 2s 4p^3 P$ upper term. The lower terms are $1s^2 2s 3s^3 S$ and $1s^2 2s 3d^3 D$. The transition probabilities⁶ are 1.5×10^9 and $5.4 \times 10^8 \text{ sec}^{-1}$, respectively. The relative calibration accuracy is expected to be $\pm 17\%$ over this entire range.

Before discussing the results, it is important to clarify some nomenclature used for the spectroscopic terms involved. For neonlike Ar^{8+} and Cl^{7+} the use of *LS* coupling is quite common and descriptive. For higher-*Z* elements (e.g., in the x-ray laser literature), *jj*-coupling designations are more appropriate. The correspondence with *jj* terms for five of the more intense (lasing) lines (*A-E*) observed are given in the footnotes to Table I. Sometimes ambiguities arise in *LS* notation. For example, strong mixing occurs between the $3p^1 D_2$ and $3p^3 P_2$ terms, resulting in reverse designations by some authors. We have followed the convention of Buchet *et al.*,⁷ our main source for wavelengths. However, Jupén,⁸ from whom we also draw data, uses the opposite *LS* designations for these two terms.

For the theoretical model, steady-state equilibrium equations are set up for the neonlike ionic species and solved for level populations. Neighboring ionic species are

TABLE I. Ar^{8+} data vs theory for $2p^5 3p-2p^5 3s$ transitions.

Label	Levels	Wavelength (Å)	I_{theor}	I_{expt}	$I_{\text{expt}}/I_{\text{theor}}$
<i>A</i> ^a	$^1S_0-^1P_1$	468.88	41	30	0.73
<i>N</i>	$^3P_1-^3P_2$	589.4	1.9	1.9	1.0
<i>P</i>	$^3P_1-^1P_1$	692.76	Blended with <i>R</i> transition		
<i>J</i>	$^1D_2-^3P_2$	642.3	13	11	0.85
<i>B</i> ^b	$^1D_2-^3P_1$	670.8	7.4	9.1	1.2
<i>K</i>	$^1P_1-^3P_0$	691.2	3.9	2.9	0.74
<i>R</i>	$^3D_2-^3P_2$	692.7	7.6 ^c	10 ^c	1.3 ^c
<i>E</i> ^d	$^3D_2-^3P_1$	725.82	8.5	8.9	1.1
<i>D</i> ^e	$^3D_1-^3P_1$	696.48	4.7	6.1	1.3
<i>C</i> ^f	$^3P_2-^1P_1$	697.67	Blended with <i>G</i> transition		
<i>G</i>	$^3D_3-^3P_2$	697.6	40 ^g	28 ^g	0.70 ^g

^a $(2p^1/2, 3p_{1/2})_0 - (2p^1/2, 3s_{1/2})_1$.

^b $(2p^3/2, 3p_{3/2})_2 - (2p^3/2, 3s_{1/2})_1$.

^c Includes *P* transition blending.

^d $(2p^3/2, 3p_{1/2})_2 - (2p^3/2, 3s_{1/2})_1$.

^e $(2p^3/2, 3p_{3/2})_1 - (2p^3/2, 3s_{1/2})_1$.

^f $(2p^1/2, 3p_{3/2})_2 - (2p^1/2, 3s_{1/2})_1$.

^g Includes *C* transition blending.

not included as the measurements are time resolved and the data are limited to the neonlike emission interval.⁵ Collisional and radiative rates between 37 levels are calculated in intermediate coupling. It is not necessary to include energy levels of principal quantum number > 3 for the temperatures present and for comparison with temporally isolated data. In any case the effect would be small.⁹ The scattering problem is solved in the distorted-wave approximation including configuration interactions by using the SUPERSTRUCTURE program developed at the University College, London.¹⁰ Relativistic corrections are included as a perturbation to the nonrelativistic Hamiltonian. Proton-induced collisional rates are included, using a semiclassical approach¹¹ but are of minor importance for the intensities. Spectral-line intensities are obtained from the computed level populations, transition rates, and energies. From comparisons of calculations,¹² the accuracy of the predicted relative intensities is expected to be $\pm 20\%$. It is not necessary to specify the absolute ion (ground-state) density, since it cancels in the comparison of relative line intensities.

The measured relative intensities are normalized to theory for a best overall fit. All measurable line intensities from the thirty $3p-3s$ and $3d-3p$ transitions in Fig. 1 then agree with the model predictions within a factor of 2. The more intense (and hence more reliable) lines agree within $\pm 30\%$, as indicated in Tables I and II. For Ar^{8+} , the comparison with theory is illustrated for these lines in the partial spectrum in Fig. 3. The important *C* (laser) line is unfortunately masked by the stronger *G* line. However, it was possible to compare the *C* intensity with those of *A*, *B*, and *D* for Cl^{7+} , as shown in Table II.

The Ar^{8+} wavelengths in Table I are taken from experimental data.⁷ The experimental wavelengths for Cl^{7+} in

TABLE II. Cl^{7+} data vs theory for $2p^5 3p-2p^5 3s$ transitions.

Label	Levels	Wavelength (\AA)	I_{theor}	I_{expt}	$I_{\text{expt}}/I_{\text{theor}}$
A	$^1S_0-^1P_1$	528.96	99	77	0.78
B	$^1D_2-^3P_1$	754.26	13	14	1.1
C	$^3P_2-^1P_1$	788.0	19	21	1.1
D	$^3D_1-^3P_1$	783.43	9.9	12	1.2

Table II are obtained from Ref. 8. The measured relative intensities I_{expt} are normalized to a best overall fit compared to the theoretical values I_{theor} . The overall precision of the measured intensities is estimated to be $\pm 25\%$. The ratio of the theoretical and experimental intensities are compared in the last column of each table. The $\pm 30\%$ agreement is the same as the combined accuracy of the experimental and theoretical values, estimated separately above.

In summary, none of the extreme ultraviolet spectral lines from thirty transitions measured for neonlike Ar^{8+} and Cl^{7+} ions show a difference in relative intensity greater than a factor of 2, compared to the predictions of a numerical model. Furthermore, the 15 stronger lines, including the lines shown to lase, agree with the model within $\pm 30\%$. In particular, measured intensities from the B and C transitions, for which the upper level has $J=2$ and for which unusually high gain have been measured, are not larger than predicted. Also, the A line (upper level $J=0$), for which unexpectedly low gain has been measured,² has a relatively large measured intensity here, as predicted. From these results it appears that there are no significant population irregularities, com-

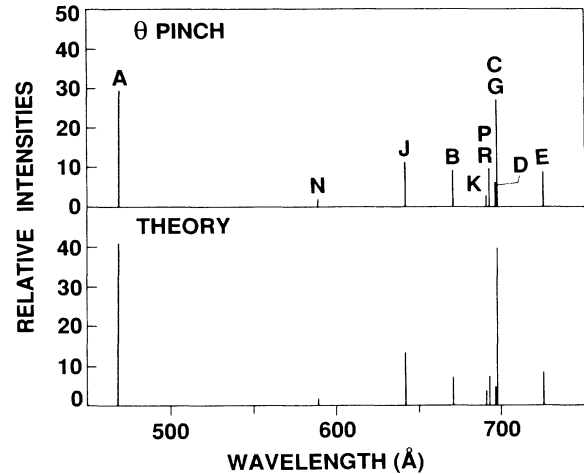


FIG. 3. Comparison of partial spectra: the upper is measured from the θ pinch, and the lower is computed. The letters refer to transitions shown in Fig. 1.

pared to the numerical model for electron-collisional excitation pumping.

The authors are grateful to J. Sugar, of the National Institute of Standards and Technology (NIST) for providing the transition probabilities needed for the branching ratio calibration. Valuable discussions with H. R. Griem and M. Blaha of the University of Maryland are also recalled with appreciation. This research was performed at the NIST while one author (R.C.E.) was a guest on sabbatical leave. This work was supported in part by the Strategic Defense Initiative Office.

¹M. D. Rosen *et al.*, Phys. Rev. Lett. **54**, 106 (1985); D. L. Matthews *et al.*, *ibid.* **54**, 110 (1985); T. N. Lee, E. A. McLean, and R. C. Elton, *ibid.* **59**, 1185 (1987).

²D. L. Matthews *et al.*, J. Phys. (Paris) **47**, 1 (1986); J. Opt. Soc. Am. B **4**, 575 (1987); R. A. London, M. D. Rosen, M. S. Maxon, and D. C. Eder, J. Phys. B (to be published).

³R. U. Datla and J. R. Roberts, Phys. Rev. A **28**, 2201 (1983).

⁴R. U. Datla and H.-J. Kunze, Phys. Rev. A **37**, 4614 (1988).

⁵R. C. Elton, R. U. Datla, J. R. Roberts, and A. K. Bhatia, Phys. Scr. (to be published).

⁶J. Sugar (private communication). These transition probabilities were calculated with the Cowan Hartree-Fock code which includes relativistic corrections. For further details, see R. D. Cowan, *The Theory of Atomic Structure and Spectra* (Univ.

of California Press, Berkeley, 1981).

⁷J.-P. Buchet *et al.*, J. Phys. B **20**, 1709 (1987).

⁸C. Jupén, Phys. Scr. **36**, 776 (1987).

⁹H. Zhang, D. H. Sampson, R. E. H. Clark, and J. B. Mann, At. Data Nucl. Data Tables **37**, 17 (1987); D. H. Sampson (private communication).

¹⁰W. Eissner and M. J. Seaton, J. Phys. B **5**, 2187 (1972); W. Eissner, M. Jones, and H. Nussbaumer, Comp. Phys. Commun. **8**, 270 (1974).

¹¹S. O. Kastner and A. K. Bhatia, Astron. Astrophys. **71**, 211 (1979).

¹²P. L. Dufton, A. E. Kingston, and N. S. Scott, J. Phys. B **16**, 3053 (1983); G. P. Gupta, K. A. Berrington, and A. E. Kingston, J. Phys. B (to be published).